

SUPPLEMENTARY INFORMATION

**Alkanolamines as Dual Functional Solvents for Biomass
Deconstruction and Bioenergy Production**

Ezinne C. Achinivu,^{a,b} Skye Frank,^{a,c} Nawa Raj Baral,^{a,c} Lalitendu Das,^a Mood Mohan,^a Peter Otoupal,^{a,b} Emara Shabir,^{a,b} Sean Utan,^{a,b} Corinne D. Scown,^{a,c} Blake A. Simmons,^{a,c} John Gladden*^{a,b}

^aJoint BioEnergy Institute, Lawrence Berkeley National Laboratory, 5885 Hollis St, Emeryville, CA 94608, USA.

^bSandia National Laboratories, 7011 East Ave, Livermore, CA 94551, USA.

^cBiological Systems and Engineering Division, Lawrence Berkeley National Laboratory, Berkeley, CA 94720, USA.

*Corresponding Author

E-mail: jmgladden@lbl.gov; jmgladd@sandia.gov (J. M. Gladden)

PRELIMINARY SCREENING	3
Survey of Different Alkanolamines for Biomass Pretreatment	3
Pretreatment Effectiveness for Different Biomass Types	6
PROCESS DEVELOPMENT	7
Process Optimization using Design of Experiment (DOE) and Statistical Analyses	7
Scale Up/Process Consolidation	6
BIOMASS CHEMICAL AND STRUCTURAL CHARACTERIZATION	8
PXRD	8
TGA	10
FTIR	12
NMR	14
BIOCONVERSION	16

PRELIMINARY SCREENING

Survey of Different Alkanolamines for Biomass Pretreatment

Table S1. List of the alkanolamines studied and a comparison of their constituents, functional groups, and degree of substitution.

Alkanolamine	#O-H	#N-H	#H-bonds
ethanolamine	1	1 (1°)	3
1-amino-2-propanol	1	1 (1°)	3
2-(Methylamino)ethanol	1	1 (2°)	2
N, N-dimethylethanolamine	1	1 (3°)	1
1,3-diamino-2-propanol	2	1 (1°)	4
2-amino-1,3-propanediol	1	2 (1°)	5

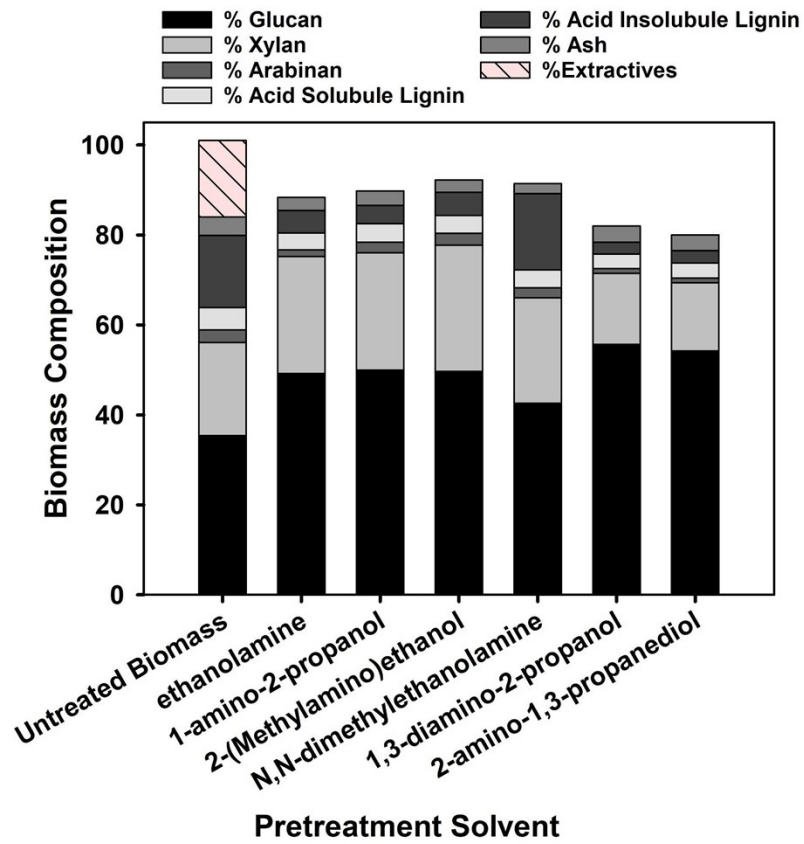


Figure S1. Biomass yield and composition after pretreatment of sorghum with the organic solvents. The composition of the untreated “raw biomass” is also displayed.

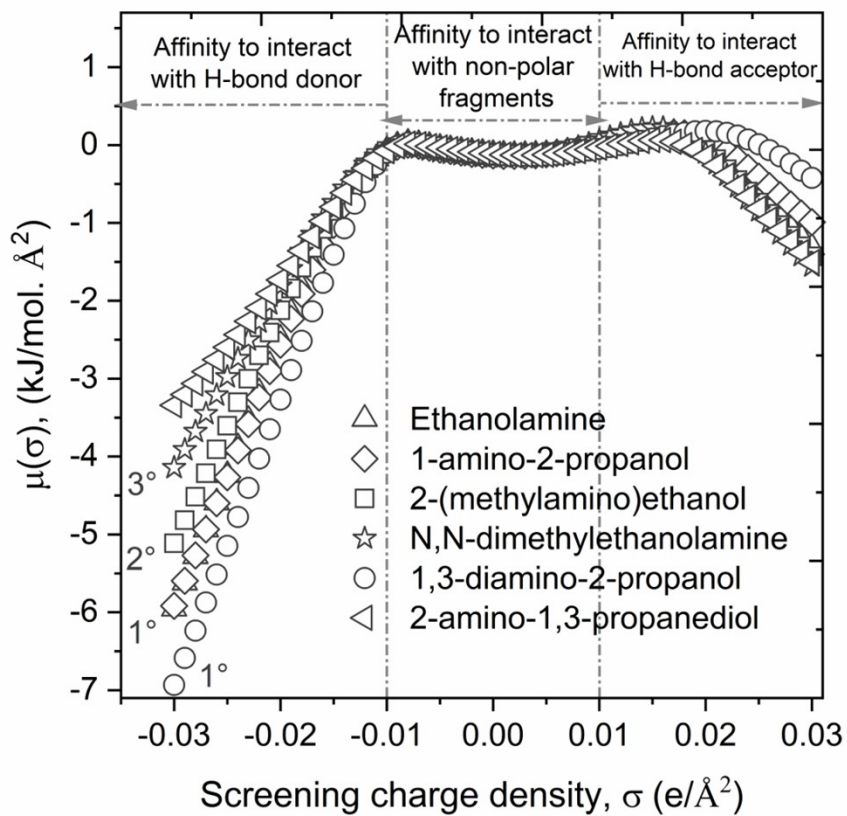


Figure S2. COSMO-RS-based predicted sigma potentials for the alkanolamines.

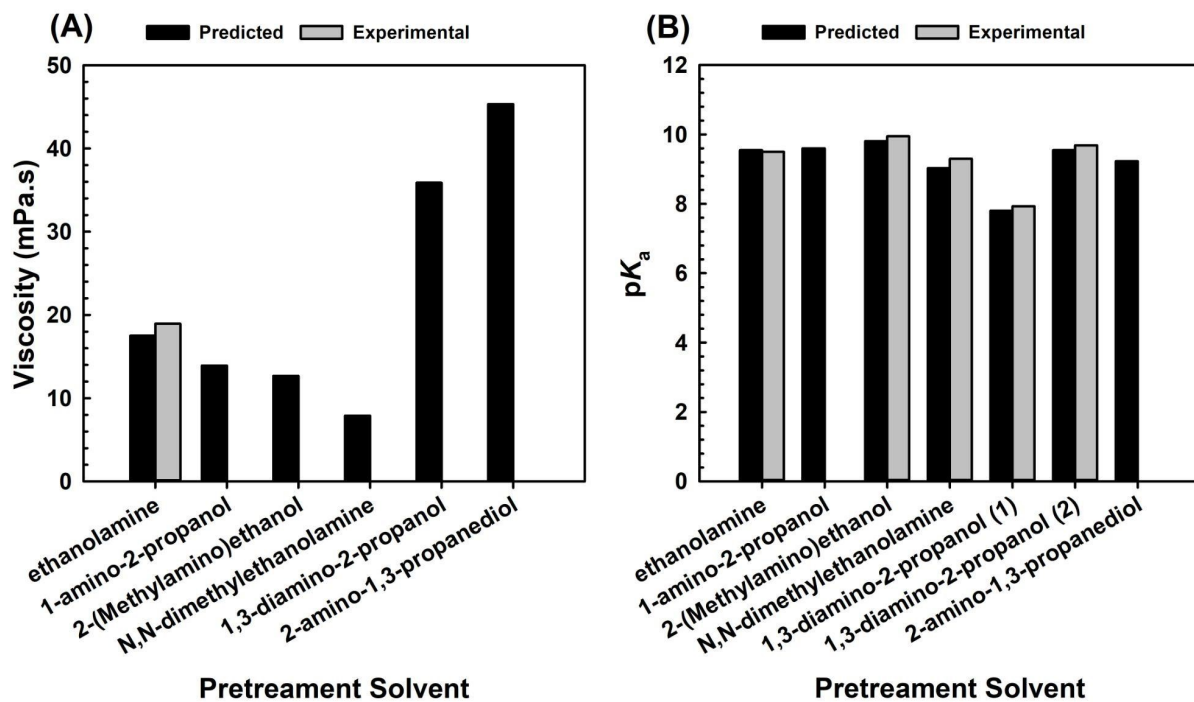


Figure S3. Predicted excess viscosities (A) and pKa values (B) for the alkanolamines screened.

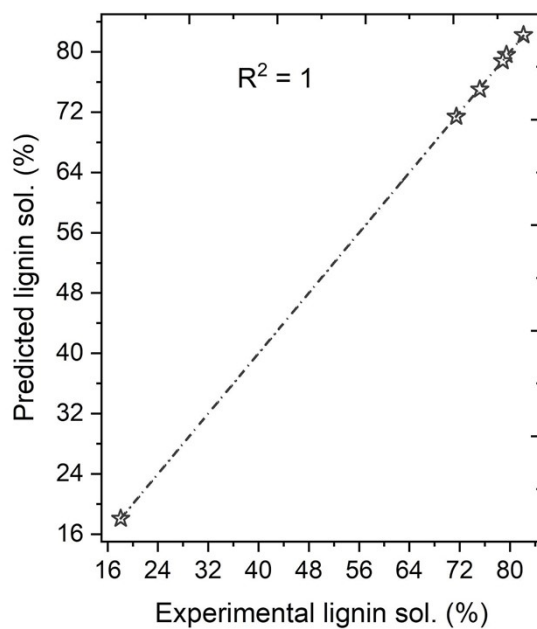


Figure S4. Experimental and COSMO-RS-based predicted lignin solubility for alkanolamines.

Pretreatment Effectiveness for Different Biomass Types

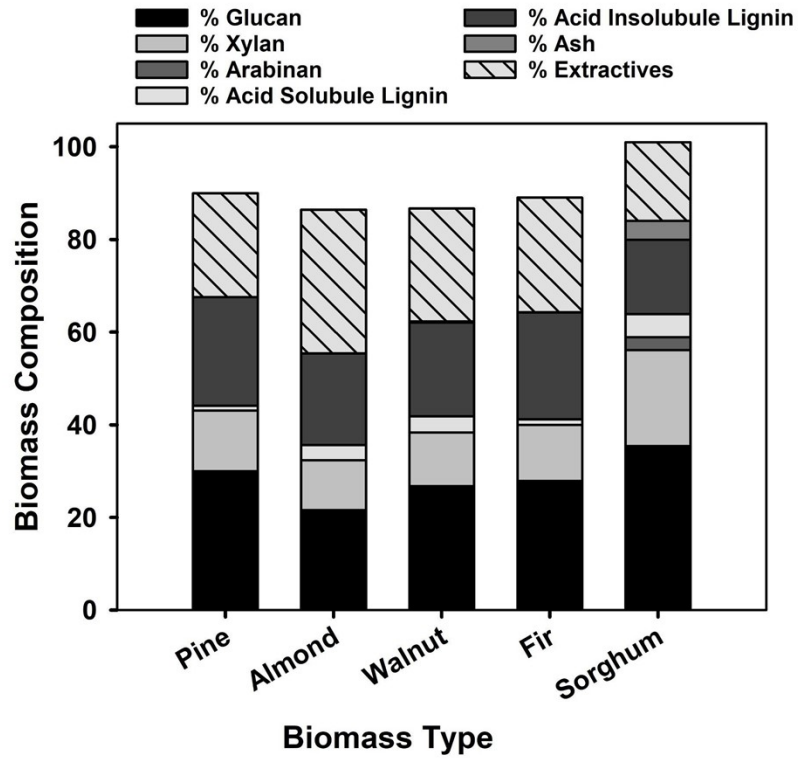


Figure S5. Biomass compositional analysis for various raw biomass types after pretreatment (and washing).

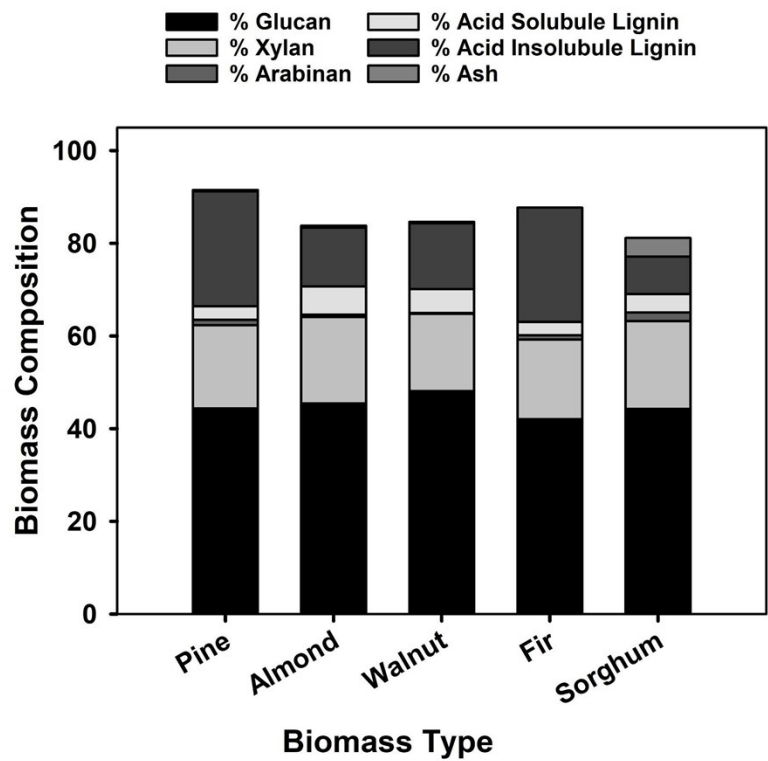


Figure S6. Biomass compositional analysis for various biomass types after pretreatment (and washing) for raw biomass.

PROCESS DEVELOPMENT

Process Optimization using Design of Experiment (DOE) and Statistical Analyses

The quadratic regression models for the glucose yield, xylose yield, lignin retained, and solid recovery were shown below:

$$\begin{aligned} \hat{Y}_{glucose} &= 87.70 + 0.14 \times time - 0.59 \times temperature + 0.42 \times solid\ loading - 1.55 \times time * time - 3.33 \\ &* temperature - 0.05 \times solid\ loading * solid\ loading - 2.77 \times temperature * time - 0.91 \\ &\times solid\ loading * time - 0.17 \times solid\ loading \\ &* temperature \end{aligned} \quad (Eq.2)$$

$$\begin{aligned} \hat{Y}_{xylose} &= 69.46 - 1.30 \times time - 0.85 \times temperature + 4.79 \times solid\ loading - 0.27 \times time * time - 2.25 \\ &* temperature + 0.13 \times solid\ loading * solid\ loading - 1.98 \times temperature * time - 0.21 \\ &\times solid\ loading * time + 0.27 \times solid\ loading \\ &* temperature \end{aligned} \quad (Eq.3)$$

$$\begin{aligned} \hat{Y}_{lignin\ removed} &= 72.55 + 3.29 \times time + 5.92 \times temperature - 3.10 \times solid\ loading - 1.07 \times time * time + 0.58 \\ &\times temperature * temperature - 0.11 \times solid\ loading * solid\ loading - 1.99 \times temperature \\ &* time + 0.29 \times solid\ loading * time + 0.48 \times solid\ loading \\ &* temperature \end{aligned} \quad (Eq.4)$$

$$\begin{aligned} \hat{Y}_{solid\ recovered} &= 64.45 - 1.99 \times time - 4.59 \times temperature + 1.30 \times solid\ loading - 0.11 \times time * time - 1.95 \\ &\times temperature * temperature - 0.54 \times solid\ loading * solid\ loading - 0.26 \times temperature \\ &* time + 0.23 \times solid\ loading * time - 0.87 \times solid\ loading \\ &* temperature \end{aligned} \quad (Eq.5)$$

where, X_1 , X_2 , and X_3 are time, temperature, and solid loading, respectively. The coefficients with one factor (X_1 , X_2 , X_3) represent the linear effects, while the coefficients with second order term (X_1^2 , X_2^2 , X_3^2) and two-factor term (X_1X_2 , X_1X_3 , X_2X_3) represent the quadratic effect and interaction effects, respectively.

Table S2. Experimental conditions and corresponding observed and predicted yields from sorghum biomass using ethanolamine.

Experiment #	Pattern	Time (h)	Temperature (°C)	Solid loading (%)	Glucose Yield (%)	Xylose Yield (%)	Lignin removed (%)	Solid Recovery (%)	Predicted Glucose Yield (%)	Predicted Xylose Yield (%)	Predicted Lignin removed (%)	Predicted Solid Recovery (%)
1	—+	1	100	40	87.1±3.2	75.9±2.0	59.3±1.4	72.5±0.3	82.0	72.0	56.9	70.1
2	00a	2	120	13.2	87.0±1.8	62.7±2.3	79.8±1.8	60.6±1.0	86.9	61.8	77.5	60.7
3	000	2	120	30	90.0±3.1	70.5±3.0	73.0±4.5	64.4±1.0	87.7	69.5	72.5	64.5
4	000	2	120	30	86.2±3.0	69.0±3.0	72.6±1.2	64.7±2.1	87.7	69.5	72.5	64.5
5	a00	0.3	120	30	78.4±3.1	67.3±2.4	59.6±5.2	66.9±2.3	83.1	70.9	64.0	67.5
6	+++	3	100	40	90.5±5.6	76.6±5.1	69.5±2.0	68.4±1.3	85.9	72.9	68.0	67.1
7	—+	1	140	20	82.4±2.2	63.1±1.8	80.2±0.7	58.8±0.4	83.6	64.2	79.5	59.3
8	0A0	2	154	30	80.0±1.3	63.2±0.8	80.8±3.9	53.9±0.0	77.3	61.7	84.1	51.2
9	00A	2	120	46.8	83.4±1.0	73.4±1.3	61.6±9.8	64.2±0.5	88.3	77.9	67.0	65.1

10	A00	3.7	120	30	83.5±0.6	66.5±1.0	76.4±3.8	60.3±0.0	83.5	66.5	75.1	60.8
11	++-	3	140	20	78.3±1.5	56.7±0.4	81.3±2.1	52.7±0.1	80.2	58.1	81.5	54.3
12	-++	1	140	40	88.1±9.4	77.1±9.5	78.2±1.0	58.4±1.9	86.0	74.7	73.7	59.7
13	+--	3	100	20	87.7±5.0	64.5±3.7	71.4±1.5	64.3±2.4	86.6	64.3	74.6	62.3
14	---	1	100	20	83.3±1.2	65.4±0.1	65.2±2.8	67.3±0.9	79.0	62.5	64.6	66.2
15	0a0	2	86	30	71.8±1.5	59.4±1.3	64.5±2.2	63.0±0.1	79.3	64.5	64.2	66.7
16	+++	3	140	40	77.8±1.9	67.5±1.8	78.4±1.6	55.4±0.0	78.9	67.8	76.8	55.7

Table S3. ANOVA and lack-of-fit test for Glucose yield. Asterisks (*) indicate statistical significance.

Source	DF	Sum of Squares	Mean Square	F Ratio	Prob > F	R ²
Model	9	607.4306	67.4923	2.5867	0.0197*	0.68
Error	38	991.4975	26.0920			
C. Total	47	1598.9280				
Lack of Fit	5	562.04229	112.408	8.6376	<.0001*	
Pure Error	33	429.45516	13.014			
Total Error	38	991.49745				
Parameter Estimates						
Term		Estimate	Std Error	t Ratio	Prob > t 	
Intercept		87.699439	2.079236	42.18	<.0001*	
Time (1,3)		0.138268	0.798028	0.17	0.8634	
Temperature (100,140)		-0.594844	0.798028	-0.75	0.4606	
Solid loading (20,40)		0.417333	0.798028	0.52	0.6040	
Time*Temperature		-2.765146	1.042674	-2.65	0.0116*	
Time*Solid loading		-0.906962	1.042674	-0.87	0.3898	
Temperature * Solid loading		-0.171496	1.042674	-0.16	0.8702	
Time*Time		-1.55105	0.968927	-1.60	0.1177	
Temperature * Temperature		-3.329494	0.968927	-3.44	0.0014*	

Solid loading * Solid loading	-0.049444	0.968927	-0.05	0.9596
-------------------------------	-----------	----------	-------	--------

Table S4. ANOVA and lack-of-fit test for Xylose yield. Asterisks (*) indicate statistical significance.

Source	DF	Sum of Squares	Mean Square	F Ratio	Prob > F	R ²
Model	9	1321.3897	146.821	8.1883	<.0001*	0.66
Error	38	681.3611	17.931			
C. Total	47	2002.7508				
Lack of Fit	5	327.94620	65.5892	6.1244	0.0004	
Pure Error	33	353.41493	10.7095			
Total Error	38	681.36114				
Parameter Estimates						
Term		Estimate	Std Error	t Ratio	Prob > t	
Intercept		69.458431	1.72364	40.30	<.0001*	
Time (1,3)		-1.295873	0.661547	-1.96	0.0575	
Temperature (100,140)		-0.853914	0.661547	-1.29	0.2046	
Solid loading (20,40)		4.7944521	0.661547	7.25	<.0001*	
Time*Temperature		-1.975804	0.864353	-2.29	0.0279*	
Time*Solid loading		-0.205596	0.864353	-0.24	0.8133	
Temperature * Solid loading		0.2651542	0.864353	0.31	0.7607	
Time*Time		-0.274729	0.803219	-0.34	0.7342	

Temperature * Temperature	-2.24936	0.803219	-2.80	0.0080*
Solid loading * Solid loading	0.1318986	0.803219	0.16	0.8704

Table S5. ANOVA and lack-of-fit test for Lignin removed. Asterisks (*) indicate statistical significance.

Source	DF	Sum of Squares	Mean Square	F Ratio	Prob > F	R ²
Model	9	2445.2926	271.699	13.4855	<.0001*	0.76
Error	38	765.6084	20.148			
C. Total	47	3210.9010				
Lack of Fit	5	350.87726	70.1755	5.5839	0.0008*	
Pure Error	33	414.73109	12.5676			
Total Error	38	765.60836				
Parameter Estimates						
Term	Estimate	Std Error	t Ratio	Prob > t		
Intercept	72.5468	1.827095	39.71	<.0001*		
Time (1,3)	3.2905685	0.701254	4.69	<.0001*		
Temperature (100,140)	5.9221818	0.701254	8.45	<.0001*		
Solid loading (20,40)	-3.103305	0.701254	-4.43	<.0001*		
Time*Temperature	-1.990408	0.916233	-2.17	0.0361*		
Time*Solid loading	0.2916083	0.916233	0.32	0.7520		
Temperature * Solid loading	0.4835583	0.916233	0.53	0.6007		

Time*Time	-1.069359	0.851429	-1.26	0.2168
Temperature * Temperature	0.5764851	0.851429	0.68	0.5025
Solid loading * Solid loading	-0.108365	0.851429	-0.13	0.8994

Table S6. ANOVA and lack-of-fit test for Solid recovered. Asterisks (*) indicate statistical significance.

Source	DF	Sum of Squares	Mean Square	F Ratio	Prob > F	R ²
Model	9	1238.2025	137.578	31.2974	<.0001*	0.88
Error	38	167.0414	4.396			
C. Total	47	1405.2439				
Lack of Fit	5	118.24426	23.6489	15.9930	<.0001*	
Pure Error	33	48.79716	1.4787			
Total Error	38	167.04142				
Parameter Estimates						
Term		Estimate	Std Error	t Ratio	Prob > t	
Intercept		64.451849	0.853434	75.52	<.0001*	
Time (1,3)		-1.998487	0.327555	-6.10	<.0001*	
Temperature (100,140)		-4.586121	0.327555	-14.00	<.0001*	
Solid loading (20,40)		1.3012744	0.327555	3.97	0.0003*	
Time*Temperature		-0.255042	0.427971	-0.60	0.5548	
Time*Solid loading		0.2297833	0.427971	0.54	0.5945	
Temperature * Solid loading		-0.868133	0.427971	-2.03	0.0496*	
Time*Time		-0.114058	0.397701	-0.29	0.7758	
Temperature * Temperature		-1.948541	0.397701	-4.90	<.0001*	
Solid loading * Solid loading		-0.539306	0.397701	-1.36	0.1831	

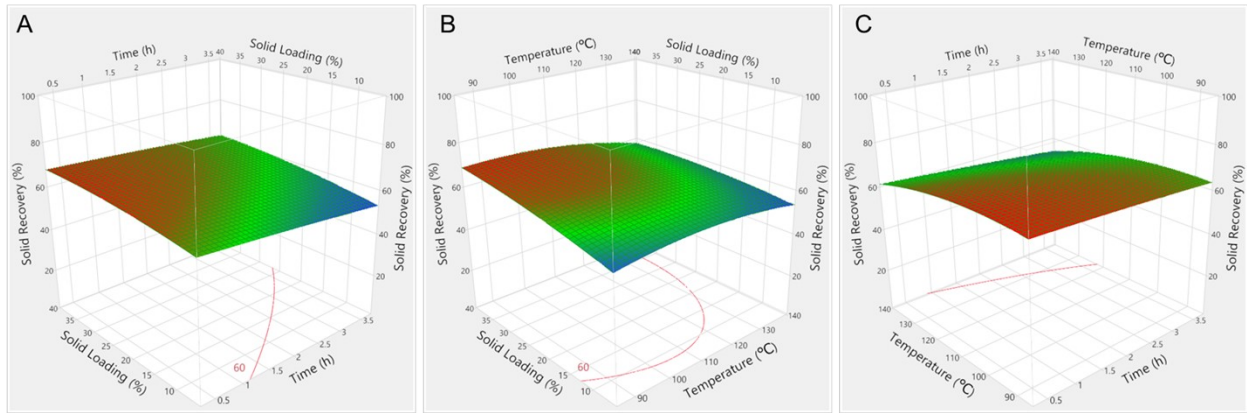


Figure S7. Surface response plots for lignin removed showing the effects of A) reaction time and solid loading, B) solid loading and temperature and C) temperature and reaction time.

Scale Up/Process Consolidation

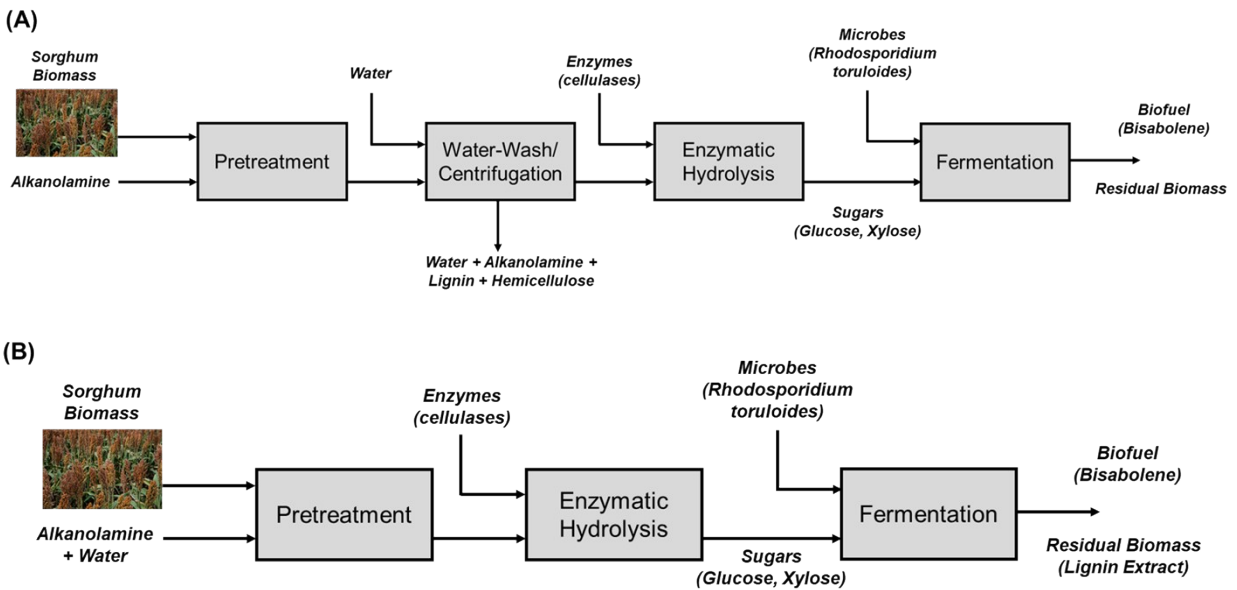


Figure S8. Process flow diagram showing a comparison between the water washing technique (A) and one pot technique (B) used in this study.

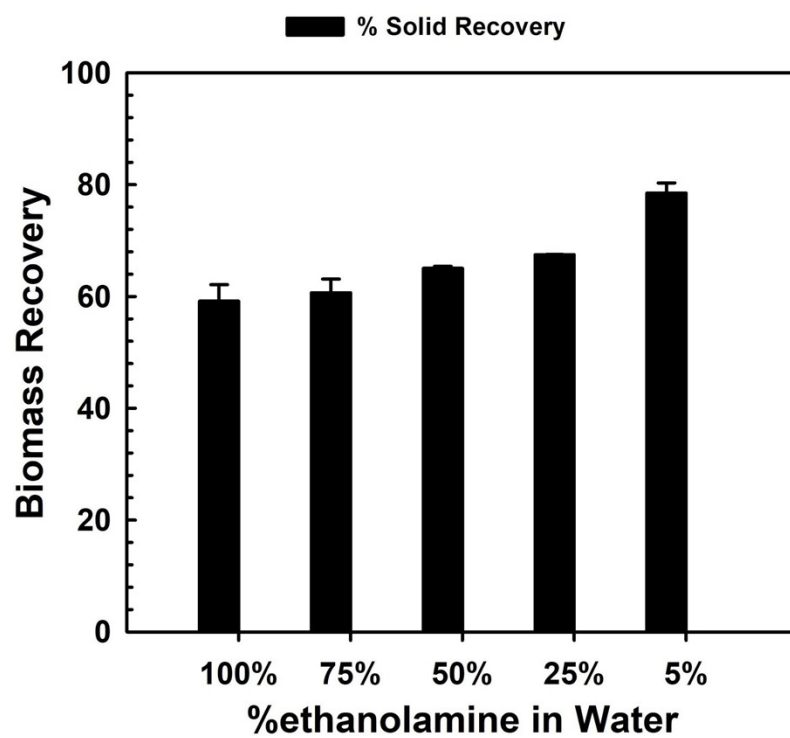


Figure S9. Solid recovery after biomass pretreatment with ethanolamine and varying amounts of water.

BIOMASS CHEMICAL AND STRUCTURAL CHARACTERIZATION

PXRD

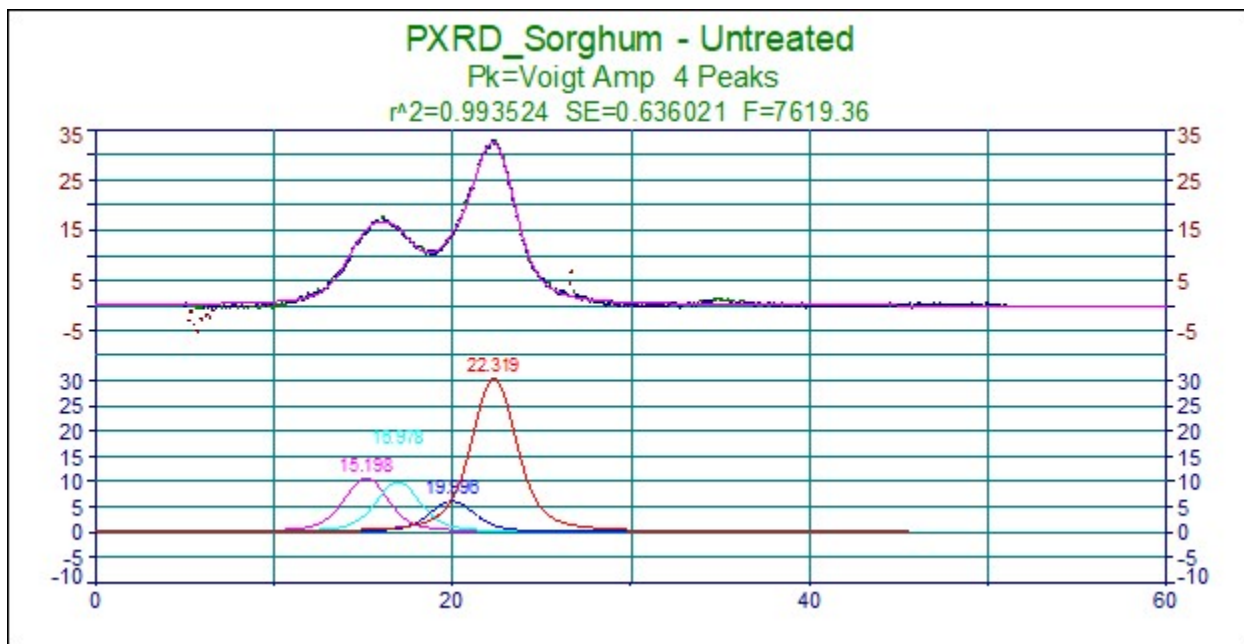


Figure S10. X-ray diffraction profiles for untreated sorghum along with results from peak deconvolution.

Table S7. X-ray diffraction profiles for untreated sorghum along with results from peak deconvolution and relative areas of each peaks

Peak	Type		Analytic Area	% Area	Int Area	% Area	Centro id	mome nt
1	Voigt	Amp	37.6925859	13.610	36.595	13.531	15.348	10.991
				7399	587	2506	1912	4303
2	Voigt	Amp	57.618387	20.805	56.111	20.747	16.958	10.990
				9187	9713	4508	3417	967
3	Voigt	Amp	28.3427634	10.234	27.695	10.240	19.796	10.992
				5321	3545	3817	8155	662

4	Voigt	Amp	153.278938	55.348	150.04	55.480	22.457	10.994
				8094	9451	9169	0233	724
Total	276.932674	100	270.452364	100				

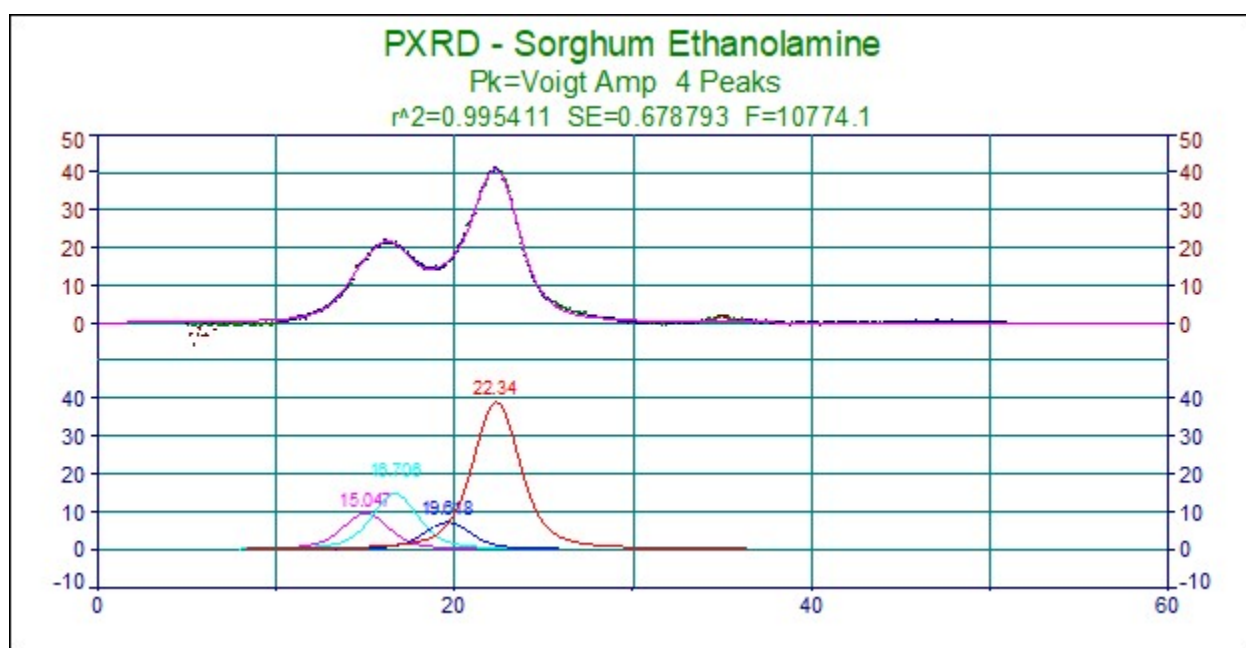


Figure S11. X-ray diffraction profiles for ethanolamine-treated sorghum along with results from peak deconvolution.

Table S8. X-ray diffraction profiles for ethanolamine-treated sorghum along with results from peak deconvolution and relative areas of each peaks

Peak	Type		Analytic Area	% Area	Int Area	% Area	Centroid	moment
1	Voigt	Amp	39.8731	18.708	38.806	18.614	15.472	10.230
			156	854	4318	6247	1664	5228
2	Voigt	Amp	36.7806	17.257	35.900	17.220	17.205	10.230

			41	8348	5095	7153	5883	2058
3	Voigt	Amp	22.8880 028	10.739 2737	22.408 6284	10.748 9452	20.153 1641	10.231 7764
4	Voigt	Amp	113.582 549	53.294 0375	111.35 7243	53.415 7148	22.428 6174	10.233 2549
Total	213.124308	100	208.472 813	100				

TGA

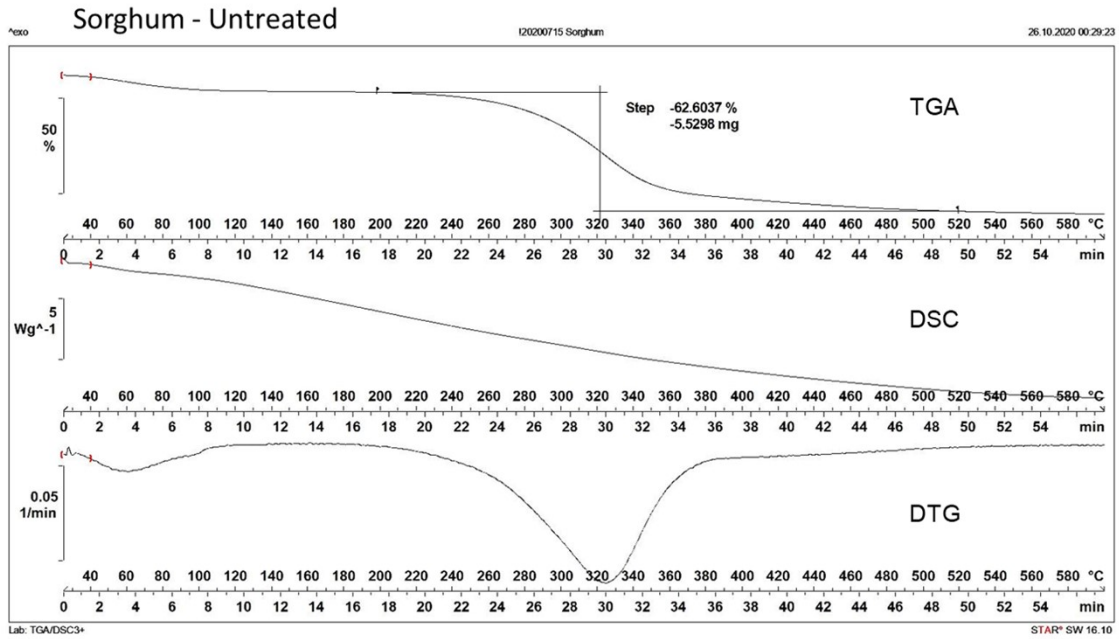


Figure S12. TGA for untreated sorghum showing the percent weight change after thermal treatment.

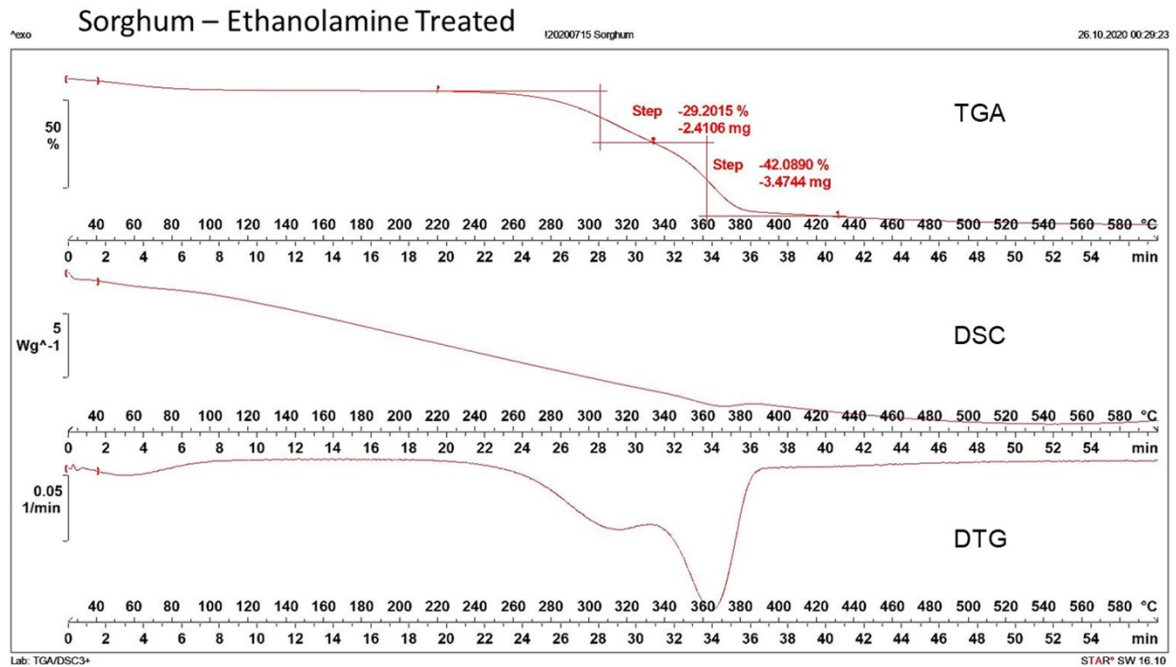


Figure S13. TGA for ethanolamine-treated sorghum showing the percent weight change after thermal treatment.

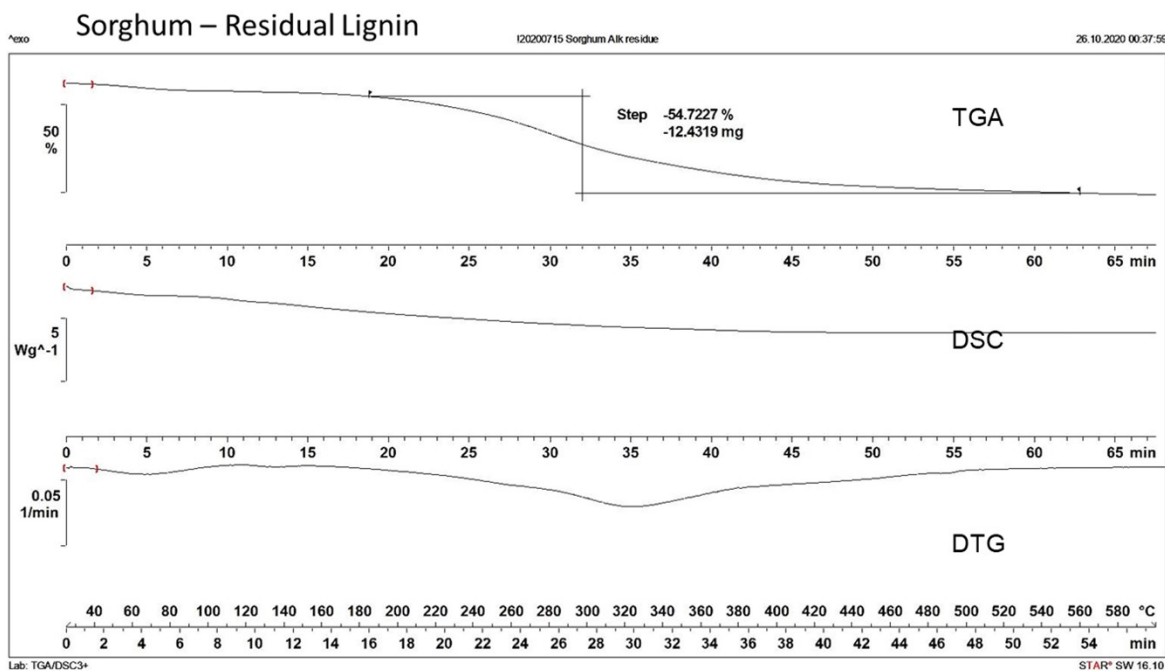


Figure S14. TGA for recovered lignin after ethanolamine-treatment of sorghum showing the percent weight change after thermal treatment.

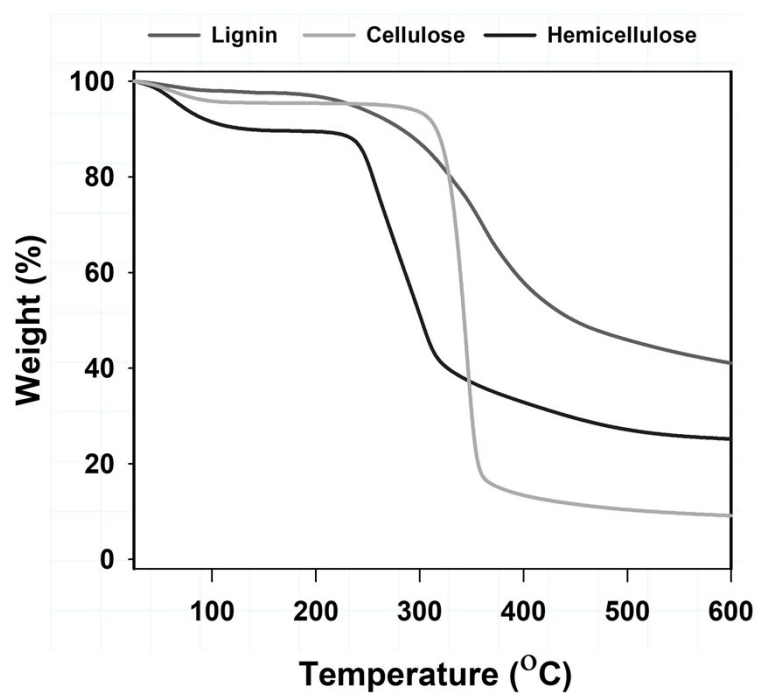


Figure S15. Thermal degradation behavior of commercially available biopolymers (xylan - hemicellulose, organosolv lignin, microcrystalline cellulose) using TGA analyses.

FTIR

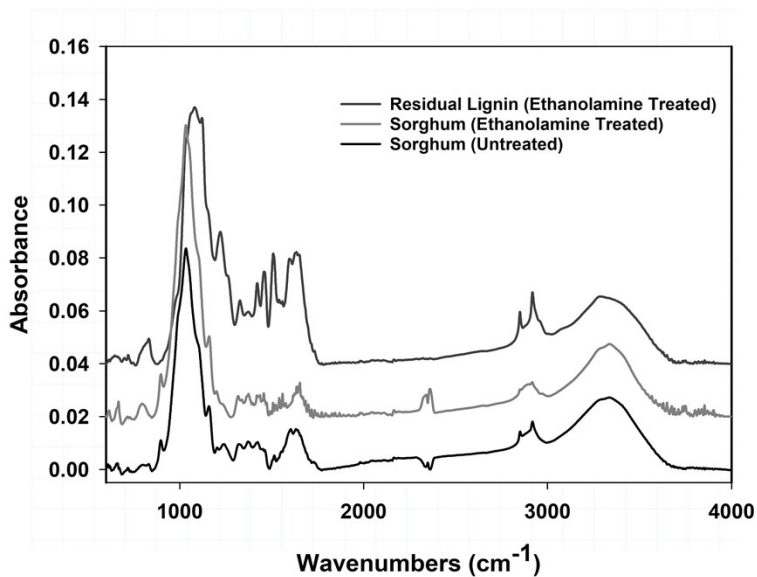


Figure S16. Complete FTIR spectra of sorghum before and after ethanolamine-based pretreatment (600–4000 cm⁻¹).

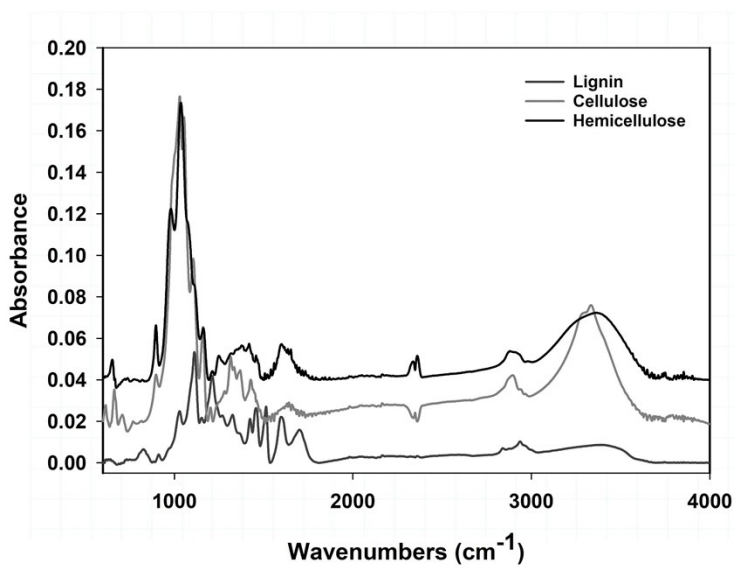


Figure S17. Complete FTIR spectra of commercially available biopolymers (xylan - hemicellulose, organosolv lignin, microcrystalline cellulose) (600–4000 cm⁻¹).

Table S9. FTIR analysis depicting the peak assignment for key functional groups in sorghum/lignin sorghum before and after ethanolamine-based pretreatment.

Wavenumber (cm ⁻¹)	Assignment
1,732	Alkyl ester from cell wall hemicellulose C=O; strong carbonyl groups in branched hemicellulose
1,710–1,712	C=O in phenyl ester from lignin
1,638–1,604	Doublet phenolics of remained lignin
1,517–1,516	Aromatic C–O stretching mode for lignin; guayacyl ring of lignin
1,453–1,456	Syringyl absorption of hardwoods (C–H methyl and methylene deformation)
1,426–1,429	C–H vibrations of cellulose; C–H deformation (asymmetric) of cellulose
1,370–1,375	C–H stretch of cellulose
1,315–1,317	C–O vibration of syringyl ring of lignin
1,242–1,247	C–O–H deformation and C–O stretching of phenolics

NMR

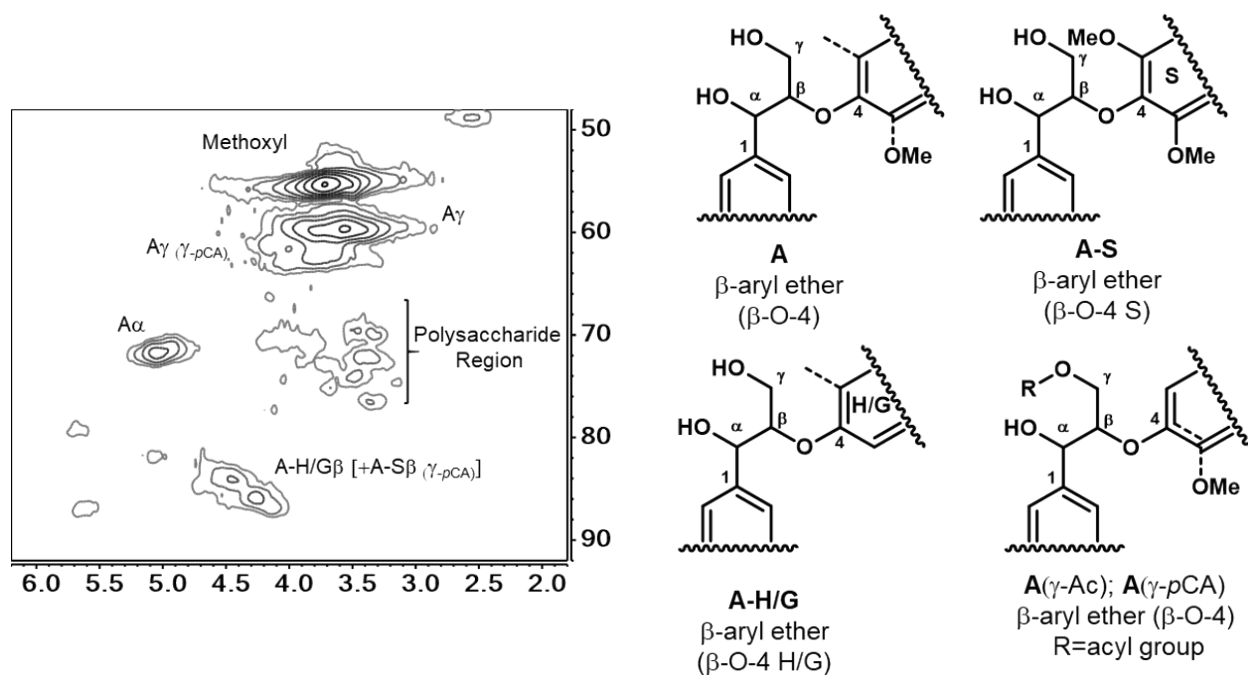


Figure S18. Lignin monomeric composition in lignin extract analyzed by 2D ^{13}C - ^1H HSQC NMR spectroscopy showing the aromatic region (~ 2.5 – $6.0/50$ – 90 ppm)). Lignin monomer ratios including tricinn (T) are provided on the figures. S: syringyl, G: guaiacyl, H: p-hydroxyphenyl, pCA: p-coumarate, FA: ferulate.

Table S10. NMR analysis depicting the peak assignment for key functional groups in sorghum/lignin sorghum before and after ethanolamine-based pretreatment.

f2 (ppm)	f1 (ppm)	Assignment		% area
8.58	147.97	Pyridine		
8.58	149.53	Pyridine		
7.72	135.47	C2–H2 and C6–H6 in p-coumarate (PCA)	H	1
7.53	137.97	Pyridine		0
7.46	129.21	C2,6–H2,6 in p-hydroxyphenyl units (H)	H	2

7.32	123.28	C2–H2 in ferulate (FA)	G	8
7.14	111.09	C6–H6 in ferulate (FA)	G	13
6.92	118.9	C5–H5 and C6–H6 in guaiacyl units (G)	G	7
6.89	114.84	C5–H5 and C6–H6 in guaiacyl units (G)	G	24
6.86	114.68	C5–H5 and C6–H6 in guaiacyl units (G)	G	23
6.85	104.06	C2–H2 and C6–H6 in etherified syringyl units (S)	S	23

5.01	71.71	C α –H α in β -O-4' substructures (A) linked to a S/G-unit
4.47	84.21	C β –H β in β -O-4' substructures (A) linked to a H-unit
4.27	85.77	C β –H β in β -O-4' substructures (A) linked to a G unit
4.18	86.55	C β –H β in β -O-4' substructures linked (A) to a S unit
4.17	61.4	C γ –H γ in γ -acylated β -O-4' substructures (A')
3.39	60.3	C γ –H γ in γ -hydroxylated β -O-4' substructures (A)

BIOCONVERSION

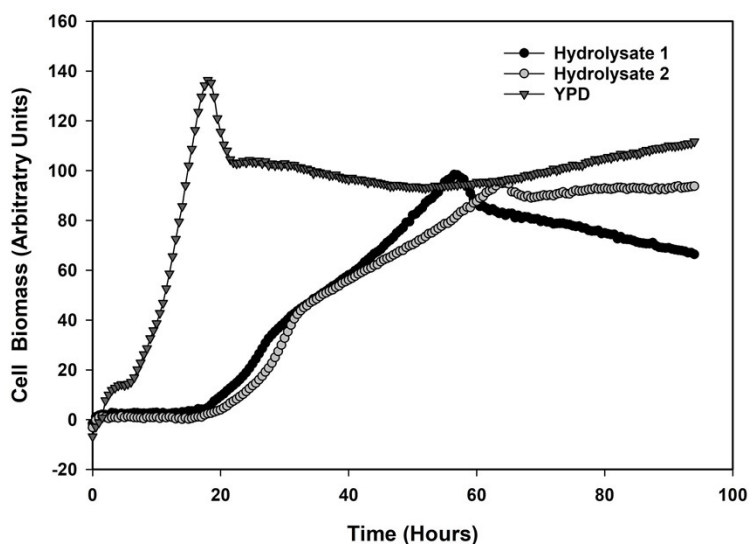


Figure S19. Growth curves of *R. toruloides* during fermentation of hydrolysate. Growth was measured using a BioLector microplate system every 30 minutes (arbitrary units). Note that BioLector measurements do not use OD₆₀₀; biomass measurements depend on buoyancy of cells which changes based on media. Error bars represent standard deviation of three technical replicates.

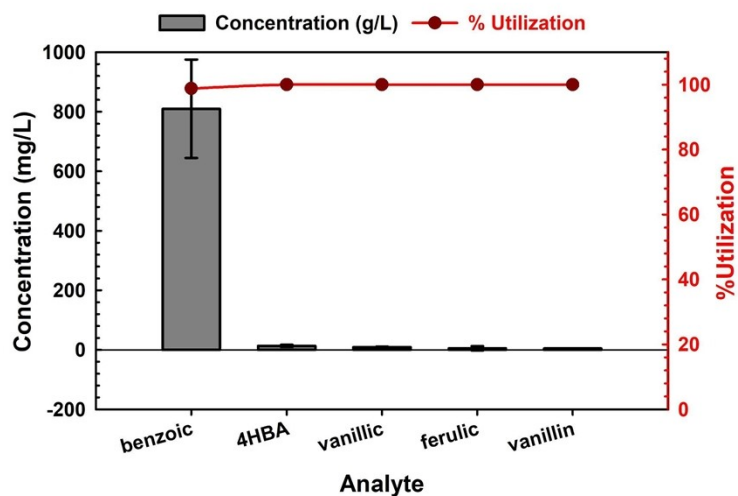


Figure S20. Average phenolic composition and utilization of each hydrolysate.

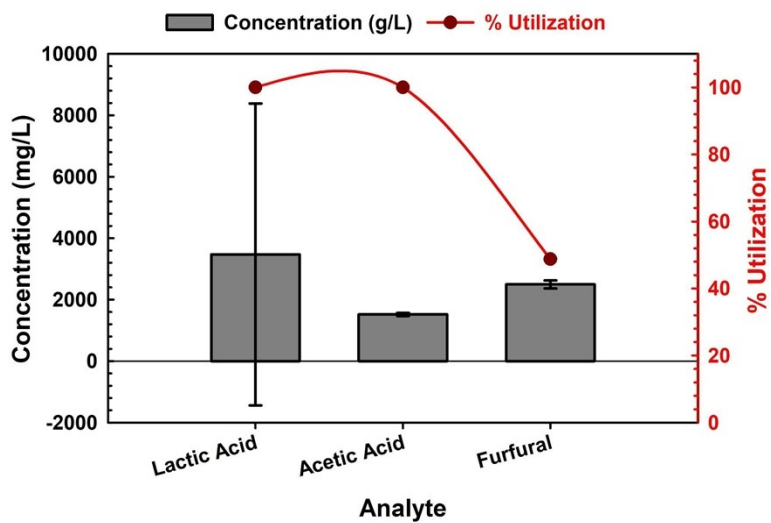


Figure S21. Average organic acid and furan composition and utilization of each hydrolysate.

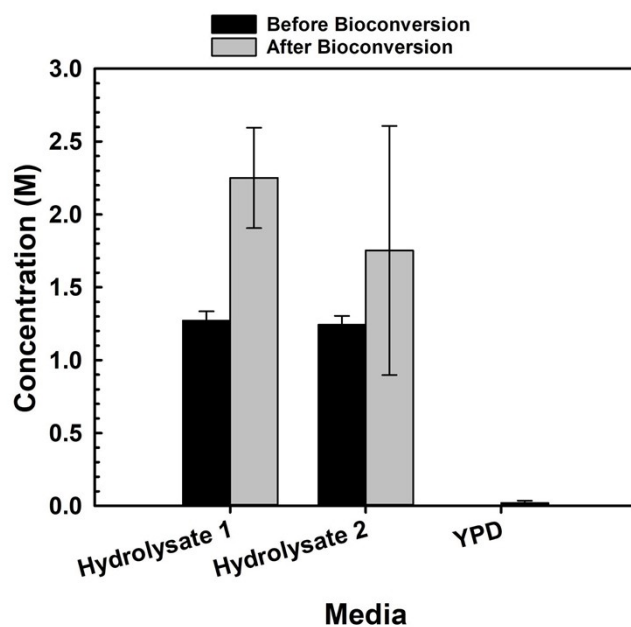


Figure S22. Average ethanolamine concentration in each hydrolysate before and after bioconversion.

There is no evidence of *R. toruloides* consuming ethanolamine. The YPD media did not contain ethanolamine. The increase in ethanolamine in the cultures is due to evaporation of water.

TECHNO ECONOMIC ANALYSIS

Table S11. Major inputs to the techno-economic model developed in this study.

Parameters	Unit	Baseline	Optimal
Biorefinery size (assumed)	t/day	2000	3000
Feedstock cost ¹	\$/t	124.6	70.0
GHG emission ¹	kgCO ₂ e/t	137.6	122.3
dLUCs ²	kgCO ₂ e/t	-46	-80
Moisture (assumed)	%	20	20
Biomass composition (Fig. 6 and prior study)³			
Acetate	wt%	2.2	0.9
Ash	wt%	4.0	2.2
Cellulose	wt%	35.4	40.0
Hemicellulose	wt%	20.7	29.8
Lignin	wt%	21.0	9.9
Protein	wt%	4.4	5.2
Pretreatment (This study)			
Solid loading rate	wt%	40	40
Solvent loading rate	wt%	15	10
Solvent cost	\$/kg	1.45	0.80
Pretreatment time	h	1	1

Enzymatic hydrolysis (This study)			
Enzyme loading rate	mg/g-biomass	10	7
Solid loading for bioconversion	wt%	14	25
Cellulose to glucose	wt%	98.63	98.63
Xylan to xylose	wt%	99.99	99.99
Hydrolysis time	h	72	48
Enzyme price ³	\$/kg-protein	5	4
Hydrolysis temperature	C	50	50
Bioconversion^{3,4}			
Corn steep liquor (CSL) cost	\$/kg	0.07	0.05
Diammonium phosphate (DAP) cost	\$/kg	0.36	0.30
CSL loading	wt%	0.25	0.20
DAP loading	g/L	0.33	0.30
Ethanol ⁴			
Bioconversion reactor power	kW/m ³	0.05	0.05
Bioconversion time	h	36.00	36.00
Glucose to ethanol	%	95.00	98.00
Xylose to ethanol	%	85.00	90.00

Bisabolene³			
Bioconversion reactor power	kW/m ³	1.50	0.56
Aeration rate	vvm	1.00	0.20
Bioconversion time	h	72.00	48.00
Glucose to bisabolene	%	5.90	90.00
Xylose to bisabolene	%	5.90	90.00
Recovery and separation^{3,4}			
Biofuel recovery	%	95	98
Solvent recovery	%	95	99
Hydrogenation³			
Hydrogen mixing rate	mol%	2.96	2.96
Hydrogen cost	\$/kg	1.61	1.25
Hydrogenation catalyst loading	wt%	0.75	0.75
Hydrogenation catalyst cost	\$/kg	261.33	231.78
Hydrogen recovery	%	85	95
Wastewater treatment⁴			
Organic matter to biogas	wt%	86	91
Onsite Energy Generation^{3,4}			

Boiler chemicals cost	\$/kg	5	4
Natural gas cost	\$/kg	0.22	0.10
Utilities^{3,4}			
Water cost	\$/kg	0.00022	0.00022
CIP (1% NaOH) price	\$/kg	0.53	0.65

Table S12. Annual operating cost

Section	Ethanol (2020\$)		Bisabolane (2020\$)	
	Current state-of-the-technology	Optimal future case	Current state-of-the-technology	Optimal future case
Feedstock supply and handling	83385798.2	70720315.1	83385798.2	70720315.1
Biomass pretreatment	23784686.5	17895901.7	23784686.5	17895901.7
Enzymatic hydrolysis	34564877.1	28598063.3	34564877.1	28598063.3
Bioconversion	10151503.6	7415301.2	37942173.4	13732193.1
Recovery and separation	13414949.0	11288197.8	29935039.4	22551361.5
Catalytic upgrading	0.0	0.0	1653606.5	13941691.9
Wastewater treatment	6887075.0	5963680.5	7035962.0	6229351.5
Onsite energy generation	7046371.0	7096962.1	28607397.8	7593132.6

Utilities	10682914.8	9075650.7	4042183.3	4552053.2
Total annual operating cost	189918175.2	158054072.4	250951724.1	185814064.0

Bibliography

- 1 N. R. Baral, J. Dahlberg, D. Putnam, J. C. Mortimer and C. D. Scown, *ACS Sustain. Chem. Eng.*, , DOI:10.1021/acssuschemeng.0c03784.
- 2 S. Gautam, U. Mishra, C. D. Scown and Y. Zhang, *Glob. Change Biol. Bioenergy*, , DOI:10.1111/gcbb.12736.
- 3 N. R. Baral, O. Kavvada, D. Mendez-Perez, A. Mukhopadhyay, T. S. Lee, B. A. Simmons and C. D. Scown, *Energy Environ. Sci.*, 2019, **12**, 807–824.
- 4 D. Humbird, R. Davis, L. Tao, C. Kinchin, D. Hsu, A. Aden, P. Schoen, J. Lukas, B. Olthof, M. Worley, D. Sexton and D. Dudgeon, *Process Design and Economics for Biochemical Conversion of Lignocellulosic Biomass to Ethanol: Dilute-Acid Pretreatment and Enzymatic Hydrolysis of Corn Stover*, National Renewable Energy Laboratory (NREL), Golden, CO (United States), 2011.